*J Appl Physiol* 124: 1025–1033, 2018.
First published January 11, 2018; doi:10.1152/japplphysiol.00530.2017.

**RESEARCH ARTICLE**

# A new role for the exhaled nitric oxide as a functional marker of peripheral airway caliber changes: a theoretical study

**Cyril Karamaoun,[1] Benoit Haut,[1] and Alain Van Muylem[2]**

[1]*Ecole polytechnique de Bruxelles, Transfers Interfaces and Processes, Université libre de Bruxelles, Brussels, Belgium; and*
[2]*Chest Department, Erasme University Hospital, Université libre de Bruxelles, Brussels, Belgium*

Submitted 6 June 2017; accepted in final form 27 December 2017

**Karamaoun C, Haut B, Van Muylem A.** A new role for the exhaled nitric oxide as a functional marker of peripheral airway caliber changes: a theoretical study. *J Appl Physiol* 124: 1025–1033, 2018. First published January 11, 2018; doi:10.1152/japplphysiol.00530.2017.—Although considered as an inflammation marker, exhaled nitric oxide ($F_ENO$) was shown to be sensitive to airway caliber changes to such an extent that it might be considered as a marker of them. It is thus important to understand how these changes and their localization mechanically affect the total NO flux penetrating the airway lumen (*Jaw*NO), and hence $F_ENO$, independently from any inflammatory status change. In this work, a new model was used. It simulates NO production, consumption, and diffusion inside the airway epithelium, NO excretion from the epithelial wall into the airway lumen and, finally, its axial transport by diffusion and convection in the airway lumen. This model may also consider the possible presence of a fluid layer coating the epithelial wall. Simulations were performed. They show the great sensitivity of *Jaw*NO to peripheral airway caliber changes. Moreover, $F_ENO$ shows distinct behaviors, depending on the location of the caliber change. Considering a bronchodilation, absence of $F_ENO$ change was associated with dilation of central airways, $F_ENO$ increase with dilation down to pre-acinar small airways, and $F_ENO$ decrease with intra-acinar dilation due to the amplification of the back diffusion flux. The presence of a fluid layer was also shown to play a significant role in $F_ENO$ changes. Altogether, the present work theoretically supports that specific $F_ENO$ changes in acute situations are linked to specifically located airway caliber changes in the lung periphery. This opens the way for a new role for $F_ENO$ as a functional marker of peripheral airway caliber change.

**NEW & NOTEWORTHY** Using a new model of nitric oxide production and transport, allowing realistic simulation of airway caliber change, the present work theoretically supports that specific changes of the molar fraction of nitric oxide in the exhaled air, occurring without any change in the inflammatory status, are linked to specifically located airway caliber changes in the lung periphery. This opens the way for a new role for $F_ENO$ as a functional marker of peripheral airway caliber change.

airway caliber; exhaled nitric oxide; functional index; modeling

## INTRODUCTION

Exhaled nitric oxide (NO) essentially results from NO produced in the airway epithelium and diffusing into the airway lumen during expiration (30). Because NO epithelial production has been shown to be triggered by type 2 airway inflammation (4), the exhaled nitric oxide was regarded mainly as a noninvasive inflammation monitoring tool in asthma (8).

However, besides inflammation, acute changes in airway caliber are also a primary feature of the asthma pathology and, for more than a decade, several works have shown that reductions of airway caliber, induced by airway challenges, lead to a dramatic decrease in the molar fraction of NO in the exhaled air ($F_ENO$) (7, 13, 21, 24). This decrease is even able to mask the impact of an ongoing inflammatory process on $F_ENO$ (12).

Moreover, different patterns of $F_ENO$ response to $\beta_2$-agonists were recently demonstrated in asthma patients (23). These distinct behaviors, i.e., stability, significant increase and significant decrease, were related to specific behaviors of ventilation distribution indices, reflecting airway caliber changes at different depths of the bronchial tree. So, besides its role as an inflammatory marker, $F_ENO$ is potentially a functional marker of the amplitude and the location of airway caliber changes.

This emphasizes the importance of understanding how the caliber and location in the bronchial tree of an airway affects the amount of NO penetrating its lumen from the surrounding epithelium. One work (36) partly tackled this issue using a model of NO transport in the lungs incorporating convection and molecular diffusion acting in realistic boundary conditions. However, although informative, this model was not designed to simulate the passage of NO from the epithelium to the airway lumen or the way the lumen caliber changes affect it.

Therefore, a new model has been developed. It realistically describes the airway tissue layers: smooth muscle, epithelium, and a fluid layer. It incorporates the possibility to modulate the caliber of the airways, and it simulates the NO transport in the airway lumen as well as in the epithelium. It was presented elsewhere in its technical and mathematical aspects (16). The present work focuses on theoretically assessing new physiological concepts, i.e., whether $F_ENO$ changes after acute maneuvers reflect the amplitude and the specific location of airway caliber changes, and thus whether $F_ENO$, besides its role as an inflammatory marker, may also be considered as a functional marker.

## METHODS

The detailed mathematical features of the model used in this paper are described extensively in Karamaoun et al. (16). This model integrates NO production and transport inside the epithelium, the muscle and the fluid layers, the excretion from the epithelium to the airway lumen, and the axial transport of NO in the lumen, with the last

Address for reprint requests and other correspondence: A. Van Muylem, Chest Department, Erasme University Hospital, Université libre de Bruxelles, 808 Route de Lennik, 1070 Brussels, Belgium (e-mail: avmuylem@ulb.ac.be).

  

feature being derived from Van Muylem et al. (35). The geometrical boundaries are derived from Weibel's symmetrically dichotomic model of the lung (37), which is composed of 24 generations (numbered from 0 to 23, with *generation 0* being the trachea) and associates one length and one airway diameter with each generation.

*NO production, exchange, and transport in the bronchial tissues.* An airway epithelial production is considered up to *generation 18*. Beyond that, the NO production is assumed to come from the alveolar epithelium only. From *generation 0* to *18*, the airways are assumed to be surrounded, from the outer side to the lumen side, by a blood layer, a double tissue layer representing the muscle and the epithelium, and a fluid layer, as described on Fig. 1*C*. In *generations 0* to *17*, it is assumed that NO production occurs in the bronchial epithelial layer (11) at a constant volumetric rate, written *Pr*. In *generation 18*, it is assumed that the NO production rate in the bronchial epithelial layer is equal to *Pr*/4, to yield a decrease in the total bronchial NO production in this generation when compared with the previous one, to simulate the fact that alveoli are starting to bud on the airway walls.

Once produced, a NO molecule may *1*) diffuse and be consumed in the epithelium or in the muscle layer, *2*) diffuse and be absorbed by the blood layer, which may be considered as an infinite sink due to the high affinity of NO for blood hemoglobin (6), or *3*) diffuse through the fluid layer and be excreted inside the airway lumen.

In the *i*th generation (subscript *i*), four equations describe the transport of NO in the blood (*Eq. 1*), the muscle (*Eq. 2*), the epithelium (*Eq. 3*), and the fluid (*Eq. 4*):

$$C_{t,i} = 0 \quad \text{for } x = 0, \tag{1}$$

$$D_{NO,t}\frac{d^2C_{t,i}}{dx^2} - kC_{t,i} \quad \text{for } 0 < x < \delta_M, \tag{2}$$

$$D_{NO,t}\frac{d^2C_{t,i}}{dx^2} + Pr - kC_{t,i} = 0 \quad \text{for } \delta_M < x < \delta_M + \delta_E, \tag{3}$$

and

$$D_{NO,t}\frac{d^2C_{t,i}}{dx^2} = 0 \quad \text{for} \quad \delta_M + \delta_E < x < \delta_M + \delta_E + \delta_F. \tag{4}$$

As depicted in Fig. 1*C*, the *x*-axis is a cartesian coordinate normal to the inner airway surface and originating at the muscle/blood interface; $\delta_M$, $\delta_E$, and $\delta_F$ are the muscle, epithelium, and fluid thicknesses, respectively. $C_t$ is the NO concentration in the tissue, $D_{NO,t}$ is the diffusion coefficient of NO in the tissues and in the fluid assimilated to water, and *k* is the kinetic constant of the reaction consuming NO in the epithelium and in the muscle tissues; this reaction was shown to happen mainly with superoxide and metalloproteins and to be of the first order with respect to the NO concentration (3).

These equations are written using a quasi-steady-state approximation in cartesian coordinates. These two assumptions are extensively discussed in Karamaoun et al. (16).

*Tissue-air interface.* In the airways, the tissue-air interface corresponds to $x = \delta_M + \delta_E + \delta_F$. Assuming a thermodynamic equilibrium between the NO dissolved in the tissue (concentration $C_t$) and the NO in the lumen (concentration C), the following equation can be written for the *i*th generation:

$$C_{t,i}(x = \delta_{M,i} + \delta_{E,i} + \delta_{F,i}) = \lambda_{t:air}C_i. \tag{5}$$

The equilibrium constant $\lambda_{t:air}$ is based on the Henry's constant for NO in water.

The expression of the NO flux density between the bronchial wall and the gas phase, expressed in meters per second, can thus be

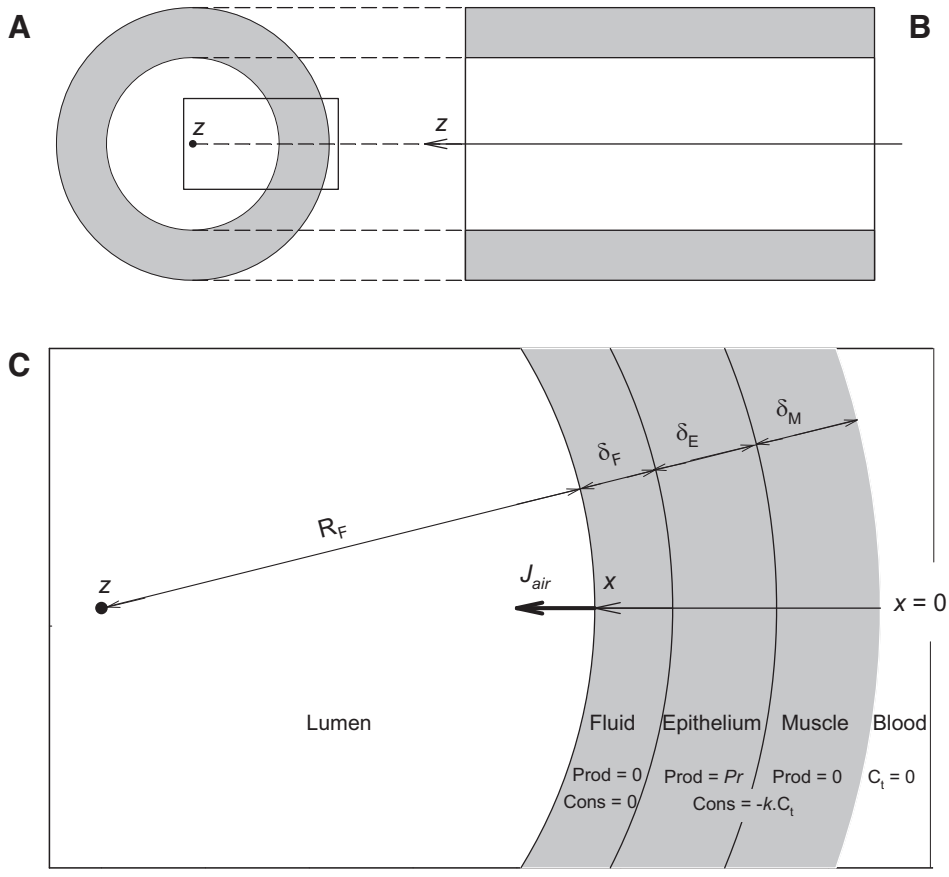


Fig. 1. Schematic representation of an airway. *A*: transversal cross-section. *B*: longitudinal cross-section. The white zone is the airway lumen; the gray zone is the airway wall. The *z*-axis is dedicated to the axial nitric oxide (NO) transport in the airway lumen. *C*: close-up of the rectangle in *A* describing the structure of the airway wall. From outer to inner part: blood (where NO tissue concentration $C_t = 0$), muscle (thickness $\delta_M$, no NO production and consumption rate equal to $-k\,C_t$), epithelium (thickness $\delta_E$, NO production rate (Prod) per unit volume equal to *Pr* and consumption (Cons) rate equal to $-k\,C_t$), and fluid (thickness $\delta_F$, no production and no consumption of NO). $R_F$ is the radius of the unobstructed part of the airway lumen. The *x*-axis is dedicated to the NO transport in the airway wall. $J_{air}$ is the flux density of NO excretion into the airway lumen.

established, based on the NO concentration gradient at the interface (30), as

$$J_{air,i} = -\gamma D_{NO,t} \frac{dC_{t,i}}{dx} \Big| (x = \delta_{F,i} + \delta_{E,i} + \delta_{M,i}), \quad (6)$$

where $\gamma$ is a dimension factor allowing for the expression of $J_{air}$ in meters per second (16).

In the alveoli, for the *i*th generation, the NO exchange flux density between the alveolar wall and the gas phase, expressed in meters per second, can be written, following Van Muylem et al. (35), as

$$J_{alv} = \left(P_{alv} - U_{alv} C_i\right) / S_{alv,tot}, \quad (7)$$

where $P_{alv}$ is the total alveolar production rate and $U_{alv}$ is the NO consumption constant in the alveolar tissues. $S_{alv,tot}$ is the total lateral surface of the alveoli, calculated from the Weibel's data (37), assuming an alveolar diameter of 0.2 mm.

*Axial NO transport in airway lumen. Equation 8* describes the axial diffusion-convection transport of the NO in the *i*th generation:

$$\frac{\partial C_i}{\partial t} = -\frac{Q_i}{\Omega_i}\frac{\partial C_i}{\partial z} + D_{NO,air}\frac{\Omega_i'}{\Omega_i}\frac{\partial^2 C_i}{\partial z^2} + \frac{1}{L_i \Omega_i}\left(J_{alv,i} S_{alv,i} + J_{air,i} S_{air,i}\right), \quad (8)$$

where z is the axial coordinate originating at the alveolar end and $t$ is the time. Q is the air flow; $\Omega$, $\Omega'$, and L are the total cross-sectional area (bronchi + alveoli), the airway cross-sectional area, and the length of the generation, respectively. $D_{NO,air}$ is the molecular diffusion coefficient of NO in air. $S_{air,i}$ and $S_{alv,i}$ are the bronchial and alveolar lateral surfaces, respectively, of the *i*th generation,. $J_{air}$ and $J_{alv}$ are the NO exchange flux densities from the airways (*Eq. 6*) and alveoli (*Eq. 7*), respectively. The model is radially expansible during a respiratory cycle. Thus Q, $\Omega'$, $\Omega$, $S_{air}$, $S_{alv,ir}$, and $J_{alv}$ are time dependent.

The hypotheses on which *Eq. 8* relies may be found in (35). Solving *Eq. 8* provides the NO concentration profile in any lung generation and for any respiratory phase.

*Airway caliber change.* This layered model is a dynamic model that can be used to simulate an airway caliber change in any bronchial generation. The outer radius of an airway is $R_F + \delta_F + \delta_E + \delta_M$, with $R_F$ being the inner radius (see Fig. 1*C*). During a bronchoconstriction, the surrounding muscle is contracting. Its shortening leads to a decrease of the outer radius and, consequently, to a decrease of the radii of each layers. Because of the volume conservation in each layer, their thicknesses ($\delta_F$, $\delta_E$, and $\delta_M$) increase, reducing the inner radius $R_F$ to a larger extent than the outer radius.

A constriction coefficient $\beta$ is defined, for the *i*th generation, as

$$\beta_i = 1 - \frac{R_{F,i}^2}{R_{F,i,0}^2} \quad (9)$$

The subscripted 0 indicates that the radius is evaluated with no bronchoconstriction occurring. Thus, $\beta$ compares the airway lumen before and after constriction, with $\beta = 0$ indicating no constriction and $\beta = 1$ indicating a total occlusion of the bronchus.

Bronchoconstrictions were simulated by comparing a baseline state ($\beta = 0$) with an obstructed state (with a given $\beta$), and bronchodilations were simulated by comparing an obstructed state (with a given $\beta$) with a nonobstructed state ($\beta = 0$). In this way, $0 < \beta < 1$ may be used to characterize the two situations.

*Numerical simulations.* The NO diffusion-convection equation (*Eq. 8*) is solved numerically in a dimensionless form to accelerate and stabilize the computations. An extensive description of the equation solving and access to the associated Wolfram Mathematica codes can be found in Karamaoun et al. (16).

The simulations were performed with a 2-s inspiratory time of a constant flow rate of 500 ml/s directly followed by a 20-s expiration at a constant flow rate of 50 ml/s. The values and dimensions of the parameters common to all generations are presented in Table 1.

The following outcomes were considered:

- The total flux of NO in the *i*th generation: $JawNO_i = J_{air,i} S_{air,i}$ (see *Eqs. 6* and *8*), at the end of expiration.
- The molar fraction of nitric oxide in the exhaled air, $F_ENO$. $F_ENO$ is defined as the NO concentration (in ppb) at the inlet of the trachea (*generation 0*), at the end of expiration. The NO production per epithelial volume Pr and the consumption coefficient *k* were adjusted to yield $F_ENO$ equal to 15 ppb in reference conditions (i.e., $\beta = 0$ and $\delta_F = 0$ in every generation).

The expiratory flow of 50 ml/s for $F_ENO$ measurement is in line with the published guidelines (2). These guidelines also recommend an inspiration up to the total lung capacity (instead of 1 liter) and $F_ENO$ measured as the mean (for at least 3 s) expiratory plateau value during an expiration of at least 6 s (instead of a single value after 20 s of expiration). The impact of the deviations from these recommendations on the calculated values of $F_ENO$ has been evaluated (35) and shown to be trivial.

## RESULTS

Table 2 summarizes the simulations, giving the parameter considered, whether or not a fluid layer or bronchoconstriction is involved, the site on which the fluid layer or the bronchoconstriction is acting, and the associated figure.

*Impacts of bronchoconstriction and fluid layer on total NO flux.* The total NO flux (*J*awNO) into the airway lumen is of primary importance as it is the source of NO enrichment of the expired gas. It is the net result of the epithelial NO production, consumption and diffusion and of the geometrical and physical properties of the epithelium-lumen interface. The simulations presented in Fig. 2 were obtained by considering a uniform bronchoconstriction ($\beta$ = constant) from *generation 0* to *gen-*

Table 1. *Parameters*

| Parameter | Description | Value | Units | Ref. No. |
|---|---|---|---|---|
| $\delta_{E,0}$ | Airway epithelium thickness | 0.0015 | cm | 10 |
| $\delta_{M,0}$ | Muscle thickness | 0.0030 | cm | 10 |
| $D_{NO,air}$ | NO diffusion coefficient in air | 0.217 | $cm^2/s$ | 35 |
| $D_{NO,t}$ | NO diffusion coefficient in tissues | $3.3\ 10^{-5}$ | $cm^2/s$ | 33 |
| $\gamma$ | Correction factor | $2.545\ 10^{4}$ | $cm^3/mol$ | 16 |
| *k* | Kinetic constant of NO consumption in the tissues | 2.001 | $s^{-1}$ | Adapted from Ref. 33 |
| $\lambda_{t:air}$ | Tissue-air equilibrium constant | $1.64\ 10^{-6}$ | $molNO{\cdot}cm^{-3}$ | Adapted from Ref. 33 |
| *Pr* | NO epithelial production per unit tissue volume | $5.61\ 10^{-12}$ | $molNO{\cdot}cm^{-3}{\cdot}s^{-1}$ | Adapted from Ref. 33 |
| $P_{alv}$ | Total NO alveolar production | $3.167\ 10^{-6}$ | mlNO/s | 25 |
| $U_{alv}$ | NO consumption constant in alveolar tissues | 1558 | $cm^3/s$ | 25 |

NO, nitric oxide.

Table 2. *Bronchoconstriction simulation summary*

| Figure | Outcome | Fluid Layer Thickness | Localization (Generation)* | Bronchoconstriction | Localization (Generation)* |
|---|---|---|---|---|---|
| Figure 2, *A* and *B* | JawNO | no | | $\beta = 0.5$; $\beta = 0.9$ | *0–18* |
| Figure 2, *C* and *D* | JawNO | 5, 10, 15μm | *0–18* | $\beta = 0.5$; $\beta = 0.9$ | *0–18* |
| Figure 3*A* | $F_ENO$ | no | | $\beta = 0.5$; $\beta = 0.9$ | *0–n*** |
| Figure 3*B* | $F_ENO$ | 5, 10, 15μm | *0–n*** | No | |
| Figure 4*A* | $F_ENO$ | 5, 10, 15μm | *0–18* | $\beta = 0.9$ | *0–18* |
| Figure 4*B* | $F_ENO$ | 5, 10, 15μm | *0–n*** | $\beta = 0.9$ | *0–18* |

JawNO, total NO flux; $F_ENO$, exhaled nitric oxide. *Generation number where fluid layer and/or bronchoconstriction are/is present; **involving all generations from *generation 0* down to a given *generation n*.

*eration 18*, with or without a fluid layer between the epithelium and the lumen.

Fig. 2*A* illustrates how a moderate ($\beta = 0.5$) and a marked ($\beta = 0.9$) constriction are acting on a single bronchiole (here of *generation 14*) without any fluid layer. The size of the red arrows is proportional to *J*awNO in each situation. Figure 2*B* shows *J*awNO as a function of the generation number in baseline ($\beta = 0$) and constricted situations ($\beta = 0.5$ and $\beta = 0.9$, in *generation 0* to *18*) without any fluid layer. The results in Fig. 2, *C* and *D*, are equivalent to those in Fig. 2, *A* and *B*, but they were obtained with a 15-μm-thick fluid layer coating the epithelium from *generations 0* to *18*. They show that this fluid layer amplifies *J*awNO decrease.

*Impacts of bronchoconstriction and fluid layer on $F_ENO$.* In the simulations presented in Fig. 3, the effect of bronchoconstriction (without fluid layer) and the effect of a fluid layer (without bronchoconstriction) on $F_ENO$ are evaluated separately. These simulations were obtained by considering either a uniform bronchoconstriction ($\beta$ = constant, $\delta_F = 0$) from *generation 0* to *generation n* or a uniform fluid layer ($\beta = 0$, $\delta_F$ = constant) from *generation 0* to *generation n*. The influence on $F_ENO$ of the depth down to which each of these effects is applied is analyzed by varying *n*.

Figure 3*A* shows $F_ENO$ change (in %baseline) when a moderate or a marked bronchoconstriction penetrates the bronchial tree (from *generation 0* up to *generation n*), tree from fluid. The baseline situation is $\beta = 0$ and $\delta_F = 0$. Figure 3*B* shows $F_ENO$ change (in %baseline) when a uniform fluid layer progressively coats the bronchial tree (from *generation 0* up to *generation n*), without muscle length change ($\beta = 0$). Different fluid layer thicknesses are considered. The baseline situation is $\delta_F = 0$ and $\beta = 0$. Noteworthy is that a 15-μm-thick fluid layer down to *generations 14* and *15* has an impact on FENO equivalent to a marked bronchoconstriction in the same area.

*Effect of the interaction between a fluid layer and bronchoconstriction on $F_ENO$.* After considering the two effects apart, the simulations presented in Fig. 4 tackle the issue of a bronchoconstriction arising in airways already coated by fluid or of a fluid layer arising in an already obstructed airway. The depth of the effect is also considered.

Figure 4*A* presents the impact of a marked bronchoconstriction ($\beta = 0.9$) progressively penetrating the bronchial tree, whereas a uniform fluid layer coats *generations 0* to *18*. Different fluid layer thicknesses (including no fluid) are considered. Figure 4*B* shows the effect on $F_ENO$ of a uniform fluid layer progressively coating the bronchial tree already markedly constricted ($\beta = 0.9$) from *generation 0* to *18*. Different fluid layer thicknesses are also considered.

*Distinct response patterns to bronchodilation.* The simulations presented in Fig. 5 are the theoretical equivalent of recent experiments (23) showing distinct patterns of $F_ENO$ change after bronchodilation, i.e., no change, increase, or decrease. These different patterns were related to different sites of drug action by specific functional tests. Three parameters are considered: the site of the bronchodilation, the amplitude ($\beta$) of the bronchodilation, and the thickness of the fluid layer.

Figure 5 summarizes the effects of an acute bronchodilation, from a baseline-constricted state (given $\beta$) to a nonconstricted

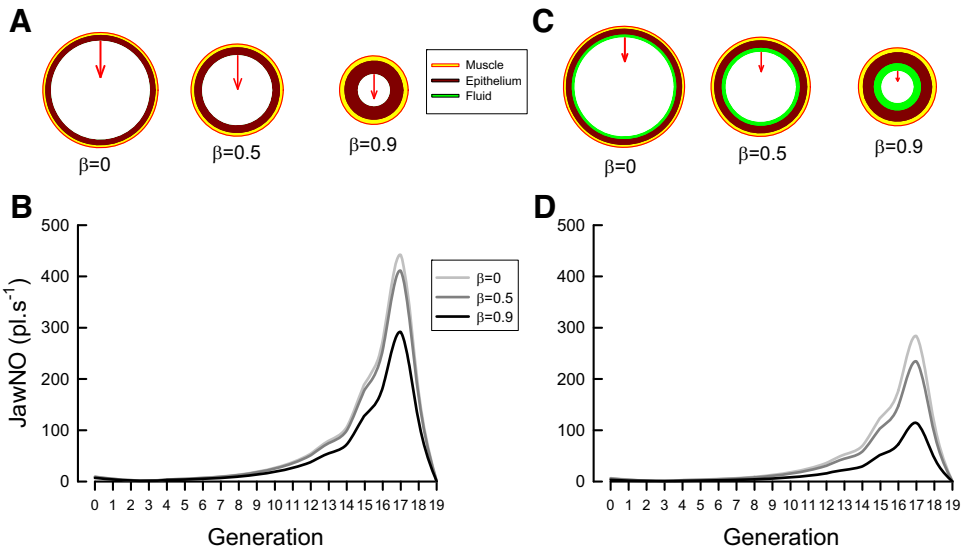


Fig. 2. *A*: cross-section of a *generation 14* bronchiole without a fluid layer, without constriction ($\beta = 0$), with a moderate constriction ($\beta = 0.5$), and with a marked constriction ($\beta = 0.9$) from *generations 0* to *18*. Red arrows are proportional to total NO flux (*J*awNO). *B*: *J*awNO as a function of the generation number for the constrictions depicted in *A*. *C* and *D*: analogous to *A* and *B*, but with a fluid layer of 15-μm thickness covering *generations 0* to *18*.

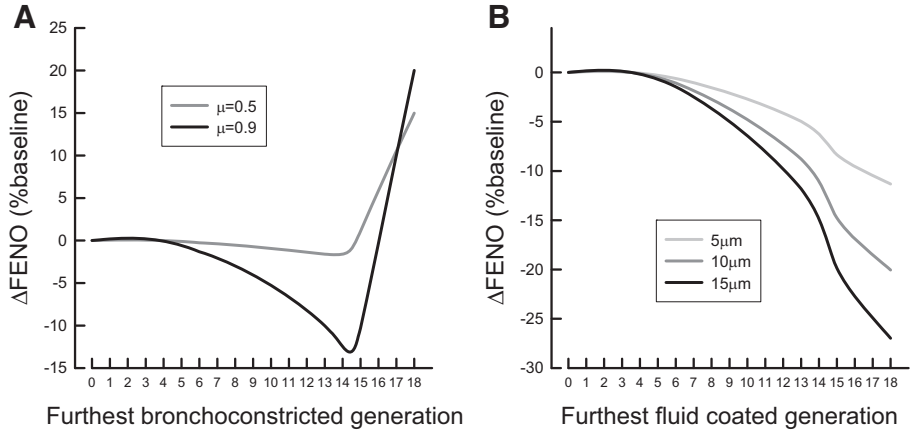


Fig. 3. *A*: exhaled nitric oxide ($F_ENO$) change (in %baseline) when a moderate (gray line) or a marked (black line) bronchoconstriction penetrates the bronchial tree (from *generation 0* up to *generation n*) free from fluid. The baseline situation is $\beta = 0$ and $\delta_F = 0$. *B*: $F_ENO$ change (in %baseline) when fluid layers of 5- (light gray), 10- (dark gray), and 15-μm (black) thickness progressively coat the bronchial tree (from *generation 0* up to *generation n*) without muscle length change ($\beta = 0$). The baseline situation is $\delta_F = 0$ and $\beta = 0$.

state ($\beta = 0$), as a function of the fluid layer thickness ($\delta_F$; abscissa) and the baseline bronchoconstriction amplitude ($\beta$; ordinate). The solid lines delineate the combinations of $\delta_F$ and $\beta$, yielding a given $F_ENO$ change (in percentage from baseline) after bronchodilation. These iso-change lines are interrupted at regular intervals by the considered value of $F_ENO$ change. By example, the lower iso-line on Fig. 5*D* corresponds to a 5% $F_ENO$ decrease and the upper line to a 15% decrease. Figure 5, *A–C*, differs by the area of the bronchial tree on which the uniform bronchodilation applies: from *generations 0* to *6* (central airways; Fig. 5*A*), *0* to *15* (up to terminal bronchioles, Fig. 5*B*), and *0* to *18* (up to intra-acinar airways; Fig. 5*C*), respectively. In the simulation presented in Fig. 5, the fluid layer coats *generations 0* to *18* (in the constricted and the nonconstricted cases). Figure 5*D* is analogous to Fig. 5*C*, but with a fluid layer coating only *generations 0* to *14* (in the constricted and the nonconstricted cases). Iso-lines are colored as a function of $F_ENO$ behavior: blue for a nonsignificant $F_ENO$ change, green for $F_ENO$ increase at least 10%, and red for $F_ENO$ decrease at least 10% after bronchodilation.

*Effect of inflammation process on $F_ENO$ and NO tissue consumption.* The simulations presented in Fig. 6 evaluate the combined effects of an increase in NO epithelial production and an overproduction of superoxides quenching NO, both of which are generated by an inflammation process. Roughly, for a 100% increase of NO epithelial production, the superoxide expression (and thus the kinetic constant *k*) experiences a two- to fivefold increase (20).

Figure 6 shows $F_ENO$ as a function of the NO epithelial production rate for a NO tissue consumption kinetic constant *k* of 2 (baseline value), 5, and 10 s. It appears that for $k = 10$ s, $F_ENO$ is 14% lower than the value calculated with $k = 2$ s.

## DISCUSSION

The simulations presented in this work theoretically support the innovative concept that $F_ENO$ may play a role as a functional marker of acute airway caliber change, not implying change in inflammatory status. Indeed, they show that caliber change may account for acute $F_ENO$ changes, as previously evidenced by experimental findings (7, 12, 13, 23, 34).

The first models of NO production and transport, notably accounting for the acute $F_ENO$ dependence on the expiratory flow rate (31), were two-compartment models, i.e., conducting airways and alveolar zone, which considered only NO transport by convection (14, 15, 25, 33). Further models (29, 35) introduced axial diffusion transport and more realistic boundary conditions based on the Weibel's symmetrical morphometric model (37). The present model (16) is the combination of a model of the axial transport of NO in the airway lumen (35) and a model of the NO diffusion inside the airway tissues surrounding the lumen, with this last model being inspired by the epithelial model developed by Tsoukias and George (33). NO produced in the epithelium is either consumed (3) or transported by diffusion to the blood surrounding the airways (considered as an infinite sink) or to the airway lumen. So,

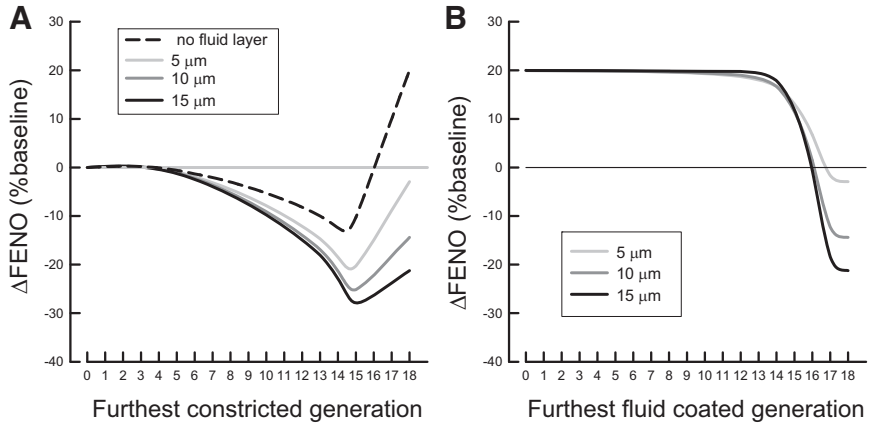


Fig. 4. *A*: $F_ENO$ change (in %baseline) due to a uniform marked bronchoconstriction ($\beta = 0.9$) penetrating the bronchial tree (from *generation 0* up to *n*) in 4 cases: *1)* $\delta_F = \delta_F^{(1)} = 5$ μm in *generations 0–18* (light gray line), *2)* $\delta_F = \delta_F^{(2)} = 10$ μm in *generations 0–18* (dark gray line), *3)* $\delta_F = \delta_F^{(3)} = 15$ μm in *generations 0–18* (black line), and *4)* without fluid [i.e., $\delta_F = \delta_F^{(4)} = 0$; dashed line]. The baseline situation of *case i* is $\beta = 0$ and $\delta_F = \delta_F^{(i)}$. *B*: $F_ENO$ change (in %baseline) due to a marked bronchoconstriction ($\beta = 0.9$) from *generations 0* to *18*, when a uniform fluid layer progressively coats the bronchial tree (from *generation 0* up to *n*). Three cases are considered: *1)* $\delta_F = \delta_F^{(1)} = 5$ μm (light gray line), *2)* $\delta_F = \delta_F^{(2)} = 10$ μm in *generations 0–18* (dark gray line), and *3)* $\delta_F = \delta_F^{(3)} = 15$ μm (black line). The baseline situation of *case i* is $\beta = 0$ and $\delta_F = \delta_F^{(i)}$ from *generation 0* to *generation 18*.

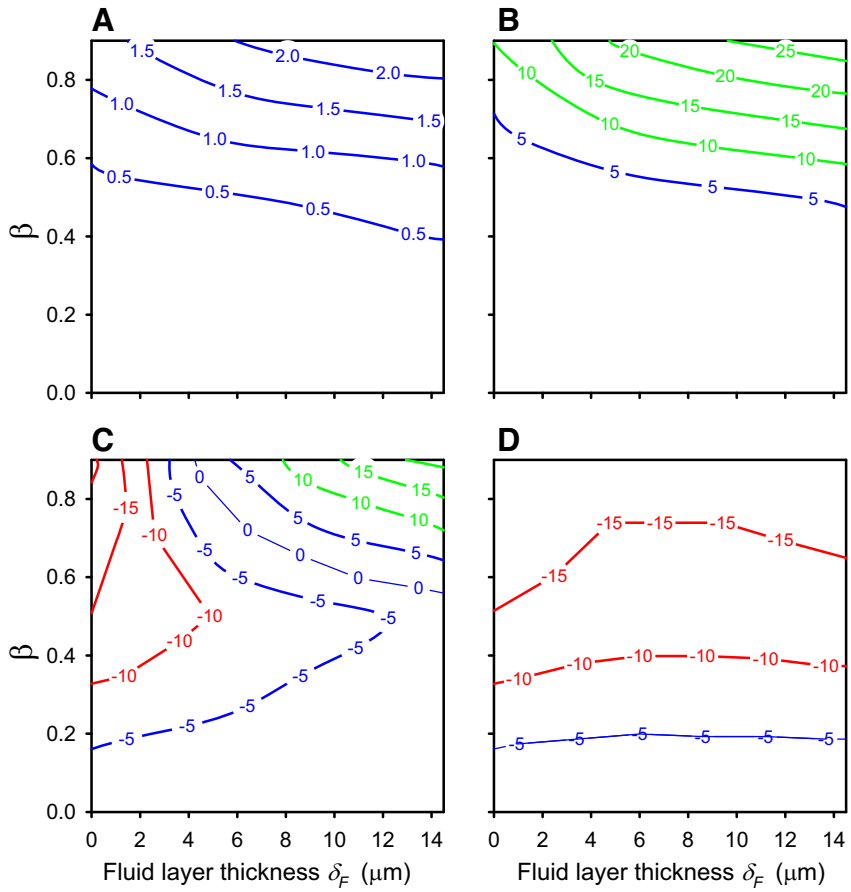


Fig. 5. Effect of an acute bronchodilation on $F_ENO$ from a baseline-constricted state to a nonconstricted state. *A–D*: contour plots of iso-$F_ENO$ change (in %baseline) as a function of the fluid layer thickness ($\delta_F$) and the baseline bronchoconstriction amplitude (β). *A*, *B*, and *C* correspond to a baseline bronchoconstriction from *generations 0* to *6*, *0* to *15*, and *0* to *18*, respectively, and a uniform fluid layer coating *generations 0–18* (in the constricted and the nonconstricted cases). *D* is analogous to *C*, but with a uniform fluid layer coating *generations 0–14* (in the constricted and the nonconstricted cases). Colored lines delineate the $\delta_F/\beta$ combinations corresponding to a nonsignificant $F_ENO$ change (blue lines), a $F_ENO$ increase (green lines), and a $F_ENO$ decrease (red lines) after bronchodilation.

instead of being imposed as in previous models, the NO flux from the epithelium into the lumen (currently called *J*awNO), which enriches alveolar air during expiration, is calculated as a function of the NO production and consumption rates inside the epithelium and of the physical and geometrical properties of the tissue and the tissue-air interface. Moreover, the present model allows evaluating the effect of an airway caliber change on *J*awNO and $F_ENO$ by simulating the shortening or lengthening (contraction and relaxation) of the muscle layer surrounding the airway. This shortening consequently impacts the thickness of the epithelial layer and its interface area with the airway lumen. A previous model tackled the issue of bronchoconstriction effect on $F_ENO$ (36). However, it was dedicated to axial NO transport and allowed only to present different scenarios, resulting from somehow arbitrary assumptions about how *J*awNO might be affected by bronchoconstriction.

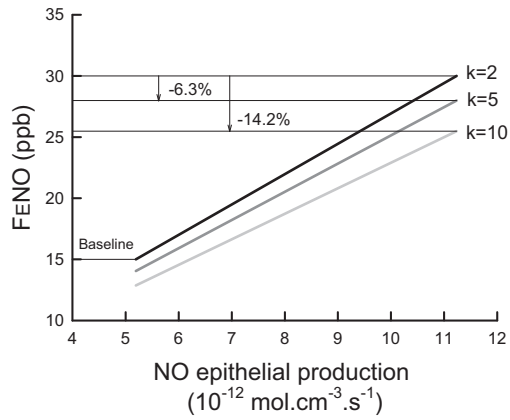


Fig. 6. $F_ENO$ as a function of the NO epithelial production rate for NO tissue consumption kinetic constants of 2 (baseline value, black line), 5 (dark gray line), and 10 (light gray line) $s^{-1}$.

The present model shows that JawNO is mechanically, i.e., without NO production change, reduced by the decrease of the available epithelial surface from which NO is excreted in the lumen, with this reduction being linked to the bronchoconstriction amplitude (see Fig. 2). Noteworthy is that this effect becomes significant only in the small airways, where the large majority of the production is concentrated. The present model also shows that a fluid layer, not considered in previous models, dramatically affects *J*awNO in the small airways (see Fig. 2).

Down to the pre-acinar small airways, i.e., in *generations 15* and *16*, $F_ENO$ decreases as a function of the bronchoconstriction amplitude and location (i.e., the deeper acts the bronchoconstriction, the larger is the $F_ENO$ decrease; see Fig. 3). This was experimentally observed with airway challenges using different provocative agents acting on different sites of the peripheral airways (23, 34), with comparable degrees of bronchoconstriction in the same subjects. When constriction penetrates deeper, the axial molecular diffusion in peripheral airways begins to play a crucial role, as already emphasized by previous models (29, 35). Indeed, during expiration, the NO concentration gradient between pre-acinar bronchioles and the

alveolar compartment induces a NO diffusion flux, the so-called "back-diffusion," toward alveoli through intra-acinar airways, removing NO molecules from the expiration flow. Acinar airway constriction impairs the back diffusion by reducing the surface through which diffusion occurs and allows more NO molecules to be expired. Consequently, $F_ENO$ increases despite an overall *J*awNO decrease (see Fig. 3).

Besides airway caliber change, a unique feature of the model used in this work is the opportunity to consider a fluid layer (assimilated to water) coating the airway epithelium. This fluid may be mucus; it may also be a water layer arising from an hypertonic saline provocation test or a sputum induction. This layer increases the length of the diffusion pathway from epithelium to the lumen, resulting in a reduction of both *J*awNO and $F_ENO$ (see Figs. 2 and 3), even when it occurred in the acinus (down to *generation 18*). Indeed, even a relatively thin layer may impair NO diffusion from the epithelium into the lumen but will not greatly affect the axial back diffusion flux. Compared with a situation without a fluid layer and for a given airway caliber reduction down to pre-acinar airways, the presence of a fluid layer amplifies $F_ENO$ decrease by 200 to 300% (see Fig. 4). Moreover, if the constriction goes deeper into the acinus, an increase of $F_ENO$ occurs only if the fluid layer is more proximal than *generations 14* and *15*, as is likely the case with the mucus layer in asthma (1, 9). With deeper fluid layer, an increase of the $F_ENO$ is not observed, even for a marked bronchoconstriction (see Fig. 4).

Although back diffusion was evidenced by heliox experiments in healthy subjects (17, 28) and in asthma patients (17), a $F_ENO$ increase due to intra-acinar caliber reduction has never been experimentally observed, likely because no currently used provocative agent has such a peripheral effect. Fortunately, the mirror maneuver, i.e., an acute bronchodilation going from a baseline-constricted state to a nonconstricted (or less constricted) state, was shown, by ventilation distribution tests, to act down to intra-acinar airways in one-third of a cohort of asthma patients. Moreover, these patients exhibited a marked $F_ENO$ decrease. The other two-thirds of asthma patients exhibited an increase or no change in $F_ENO$ (23). These observations constitute the opportunity to theoretically estimate whether simulations using different combinations of fluid thickness and bronchodilation amplitude may mimic them and whether they may be informative about the location of the bronchodilation. This is the purpose of Fig. 5. It presents, as contour plots, the combinations of fluid thickness and bronchodilation amplitude yielding a given $F_ENO$ change. These combinations were simulated for a central dilation (*generations 0–6*; Fig. 5*A*), a dilation up to pre-acinar bronchioles (*generations 0–15*; Fig. 5*B*), and a dilation up to intra-acinar airways (*generations 0–18*; Fig. 5, *C* and *D*). In Fig. 5, *A–C*, dilation is associated with fluid coating *generations 0–18* and, in Fig. 5*D*, with fluid coating only *generations 0–14*. Although some very specific β/fluid thickness combinations may lead to a nonsignificant $F_ENO$ change after peripheral bronchodilation (Fig. 5, *B* and *C*), it came out that this feature is likely associated with dilation only in central airways (Fig. 5*A*, blue lines). Conversely, a substantial $F_ENO$ change rules out a dilation limited to central airways. An increase of $F_ENO$ (Fig. 5*B*, green lines) is essentially associated with marked dilations down to pre-acinar airways, rather independently from the fluid layer thickness, but also in intra-acinar airways if a very distal fluid layer is present. A decrease in $F_ENO$ (Fig. 5, *C* and *D*, red lines) is associated only with dilation down to intra-acinar airways, even moderately, which boosts the back diffusion and thus removes NO molecules from the expiratory flow. When the fluid layer is more proximal than the 15th generation (Fig. 5*D*), as is likely the case for mucus in the asthma (1, 9), the decrease in $F_ENO$ becomes independent of the fluid layer thickness. Altogether, the present simulations confirm the link between the distinct $F_ENO$ behaviors that were experimentally evidenced after bronchodilation and specific sites of actions (23). This opens the way to a very simple and informative test, i.e., NO measurement before and after acute bronchodilation. Moreover, the simulations allow making assumptions about the presence of a fluid layer in very peripheral airways, a relevant issue out of the reach of classical lung function tests (26).

Like all model studies, this work has limitations essentially consisting in oversimplifications. We considered a constant epithelial thickness along the bronchial tree and a constant NO production per unit bronchial epithelial volume (except for *generation 18*). This may have led to overestimation of the NO production in the very peripheral airways. However, in healthy subjects, Boers et al. (5) found an increasing number of Clara cells in terminal to respiratory bronchioles, and Shaul et al. (27) showed that endothelial NO synthase is expressed in cultured cells of the same lineage as Clara cells (NCI-H441 human bronchiolar epithelial cells). This suggests an increase in NO production in peripheral airways that is likely amplified in asthma patients (34). Moreover, it comes out that the distribution of NO production assumed in the present simulations is very close to that deduced from experimental data (18, 34). All the simulations were also realized considering a (possible) fluid layer of uniform thickness. This may be acceptable for a water layer, but it is questionable for mucus. However, in the central airways, it appears that the fluid layer barely affects *J*awNO or $F_ENO$, whatever its thickness. In peripheral airways, we consider thicknesses of up to 15 μm, which may seem overestimated for mucus. Indeed, a 15-μm-thick layer would represent ±10% of a 14th generation bronchiole lumen area, where ±5% is typically described in asthma patients (1). However, in our simulations, we assimilated the fluid to water. This certainly leads to an overestimation of the NO diffusion coefficient in it. The decrease in NO diffusivity with increased mucus density, which is not yet established, should be included in further refinements of the model.

Other features may also be considered in further developments. Notably, the present model is symmetric and yields no ventilation heterogeneity. Suresh et al. (32) showed that $F_ENO$ is decreased if a substantial part of the NO production arises from a distal poorly ventilated unit in parallel with a well ventilated unit. This result is confirmed by an adapted version of our model with bronchoconstriction parameters (amplitude and location) and NO volumetric production rate possibly differing. In this model, ventilation heterogeneity between the two units is calculated according to the bronchoconstriction parameters based on classical hydraulic analysis. Simulation results show that $F_ENO$ is decreased by 30% if 70% of the NO production arises in a marked constricted distal unit (data not shown). Even if these preliminary results are interesting, it would be fruitful to associate the present model of NO production and transport with models associating ventilation de-

fects and bronchial tree asymmetry (19). Also, although the present work is focused mainly on noninflammatory effects on $F_ENO$, NO overconsumption in the lung tissues during an inflammation process is certainly worth studying. Figure 6 shows that this quenching effect (20) has to be considered, besides airway caliber and NO overproduction (22). Moreover, if induced acute bronchoconstriction may be present without inflammation, inflammation itself induces caliber changes. The present model may thus be useful to decipher these effects in the frame of asthma management.

Finally, beyond a strict modeling approach, it is to be noted that this new role of $F_ENO$ as a marker of airway caliber change after an acute intervention is theoretically not limited to asthma. $F_ENO$, a biomarker detectable even in the absence of inflammation, may be used to detect peripheral airway caliber change in other pathological situations in which $F_ENO$ is considered to have no or little usefulness as an inflammatory marker. In chronic obstructive pulmonary disease, even with active smoking, $F_ENO$ measurement before and after bronchodilation may give information about a certain degree of peripheral reversibility. In cystic fibrosis, the effect on $F_ENO$ of physiotherapy could be related to mucus displacement. These are opportunities for further developments.

In conclusion, the simulations presented in this work show that the link between the $F_ENO$ behavior after an airway caliber change and the localization (and the amplitude) of this change is theoretically sound. This opens the way for a new area of research in which $F_ENO$, besides its undeniable usefulness as an inflammation marker, may play a new role as a peripheral functional marker.

## GRANTS

This study was funded by a Microgravity Application Programme project from the European Space Agency: Airway NO in Space.

## DISCLOSURES

No conflicts of interest, financial or otherwise, are declared by the authors.

## AUTHOR CONTRIBUTIONS

C.K., B.H., and A.V.M. conceived and designed research; C.K., B.H., and A.V.M. performed experiments; C.K., B.H., and A.V.M. analyzed data; C.K., B.H., and A.V.M. interpreted results of experiments; C.K., B.H., and A.V.M. edited and revised manuscript; C.K., B.H., and A.V.M. approved final version of manuscript; A.V.M. prepared figures; A.V.M. drafted manuscript.

## REFERENCES

1. **Aikawa T, Shimura S, Sasaki H, Ebina M, Takishima T.** Marked goblet cell hyperplasia with mucus accumulation in the airways of patients who died of severe acute asthma attack. *Chest* 101: 916–921, 1992. doi:10.1378/chest.101.4.916.
2. **American Thoracic Society; European Respiratory Society.** ATS/ERS recommendations for standardized procedures for the online and offline measurement of exhaled lower respiratory nitric oxide and nasal nitric oxide, 2005. *Am J Respir Crit Care Med* 171: 912–930, 2005. doi:10.1164/rccm.200406-710ST.
3. **Beckman JS, Koppenol WH.** Nitric oxide, superoxide, and peroxynitrite: the good, the bad, and ugly. *Am J Physiol* 271: C1424–C1437, 1996. doi:10.1152/ajpcell.1996.271.5.C1424.
4. **Berry MA, Shaw DE, Green RH, Brightling CE, Wardlaw AJ, Pavord ID.** The use of exhaled nitric oxide concentration to identify eosinophilic airway inflammation: an observational study in adults with asthma. *Clin Exp Allergy* 35: 1175–1179, 2005. doi:10.1111/j.1365-2222.2005.02314.x.
5. **Boers JE, Ambergen AW, Thunnissen FB.** Number and proliferation of clara cells in normal human airway epithelium. *Am J Respir Crit Care Med* 159: 1585–1591, 1999. doi:10.1164/ajrccm.159.5.9806044.
6. **Borland CD, Higenbottam TW.** A simultaneous single breath measurement of pulmonary diffusing capacity with nitric oxide and carbon monoxide. *Eur Respir J* 2: 56–63, 1989.
7. **de Gouw HW, Hendriks J, Woltman AM, Twiss IM, Sterk PJ.** Exhaled nitric oxide (NO) is reduced shortly after bronchoconstriction to direct and indirect stimuli in asthma. *Am J Respir Crit Care Med* 158: 315–319, 1998. doi:10.1164/ajrccm.158.1.9703005.
8. **Dweik RA, Boggs PB, Erzurum SC, Irvin CG, Leigh MW, Lundberg JO, Olin AC, Plummer AL, Taylor DR; American Thoracic Society Committee on Interpretation of Exhaled Nitric Oxide Levels (FENO) for Clinical Applications.** An official ATS clinical practice guideline: interpretation of exhaled nitric oxide levels (FENO) for clinical applications. *Am J Respir Crit Care Med* 184: 602–615, 2011. doi:10.1164/rccm.9120-11ST.
9. **Fahy JV, Dickey BF.** Airway mucus function and dysfunction. *N Engl J Med* 363: 2233–2247, 2010. doi:10.1056/NEJMra0910061.
10. **Farmer SG, Hay DW.** *The Airway Epithelium: Physiology, Pathophysiology and Pharmacology*. New York: Marcel Dekker, 1991.
11. **Guo FH, De Raeve HR, Rice TW, Stuehr DJ, Thunnissen FB, Erzurum SC.** Continuous nitric oxide synthesis by inducible nitric oxide synthase in normal human airway epithelium in vivo. *Proc Natl Acad Sci USA* 92: 7809–7813, 1995. doi:10.1073/pnas.92.17.7809.
12. **Haccuria A, Michils A, Michiels S, Van Muylem A.** Exhaled nitric oxide: a biomarker integrating both lung function and airway inflammation changes. *J Allergy Clin Immunol* 134: 554–559, 2014. doi:10.1016/j.jaci.2013.12.1070.
13. **Ho LP, Wood FT, Robson A, Innes JA, Greening AP.** The current single exhalation method of measuring exhales nitric oxide is affected by airway calibre. *Eur Respir J* 15: 1009–1013, 2000. doi:10.1034/j.1399-3003.2000.01506.x.
14. **Högman M, Holmkvist T, Wegener T, Emtner M, Andersson M, Hedenström H, Meriläinen P.** Extended NO analysis applied to patients with COPD, allergic asthma and allergic rhinitis. *Respir Med* 96: 24–30, 2002. doi:10.1053/rmed.2001.1204.
15. **Jörres RA.** Modelling the production of nitric oxide within the human airways. *Eur Respir J* 16: 555–560, 2000. doi:10.1034/j.1399-3003.2000.016003555.x.
16. **Karamaoun C, Van Muylem A, Haut B.** Modeling of the nitric oxide transport in the human lungs. *Front Physiol* 7: 255, 2016. doi:10.3389/fphys.2016.00255.
17. **Kerckx Y, Michils A, Van Muylem A.** Airway contribution to alveolar nitric oxide in healthy subjects and stable asthma patients. *J Appl Physiol (1985)* 104: 918–924, 2008. doi:10.1152/japplphysiol.01032.2007.
18. **Kerckx Y, Van Muylem A.** Axial distribution heterogeneity of nitric oxide airway production in healthy adults. *J Appl Physiol (1985)* 106: 1832–1839, 2009. doi:10.1152/japplphysiol.91614.2008.
19. **Leary D, Winkler T, Braune A, Maksym GN.** Effects of airway tree asymmetry on the emergence and spatial persistence of ventilation defects. *J Appl Physiol (1985)* 117: 353–362, 2014. doi:10.1152/japplphysiol.00881.2013.
20. **Liu P, Hock CE, Nagele R, Wong PY.** Formation of nitric oxide, superoxide, and peroxynitrite in myocardial ischemia-reperfusion injury in rats. *Am J Physiol Heart Circ Physiol* 272: H2327–H2336, 1997. doi:10.1152/ajpheart.1997.272.5.H2327.
21. **Michils A, Elkrim Y, Haccuria A, Van Muylem A.** Adenosine 5′-monophosphate challenge elicits a more peripheral airway response than methacholine challenge. *J Appl Physiol (1985)* 110: 1241–1247, 2011. doi:10.1152/japplphysiol.01401.2010.
22. **Michils A, Haccuria A, Michiels S, Van Muylem A.** Airway calibre variation is a major determinant of exhaled nitric oxide's ability to capture asthma control. *Eur Respir J* 50: 1700392, 2017. doi:10.1183/13993003.00392-2017.
23. **Michils A, Malinovschi A, Haccuria A, Michiels S, Van Muylem A.** Different patterns of exhaled nitric oxide response to β2-agonists in asthmatic patients according to the site of bronchodilation. *J Allergy Clin Immunol* 137: 806–812, 2016. doi:10.1016/j.jaci.2015.09.054.
24. **Piacentini GL, Bodini A, Peroni DG, Miraglia del Giudice M Jr, Costella S, Boner AL.** Reduction in exhaled nitric oxide immediately after methacholine challenge in asthmatic children. *Thorax* 57: 771–773, 2002. doi:10.1136/thorax.57.9.771.

25. **Pietropaoli AP, Perillo IB, Torres A, Perkins PT, Frasier LM, Utell MJ, Frampton MW, Hyde RW.** Simultaneous measurement of nitric oxide production by conducting and alveolar airways of humans. *J Appl Physiol (1985)* 87: 1532–1542, 1999. doi:10.1152/jappl.1999.87.4.1532.
26. **Rogers DF.** Airway mucus hypersecretion in asthma: an undervalued pathology? *Curr Opin Pharmacol* 4: 241–250, 2004. doi:10.1016/j.coph.2004.01.011.
27. **Shaul PW, North AJ, Wu LC, Wells LB, Brannon TS, Lau KS, Michel T, Margraf LR, Star RA.** Endothelial nitric oxide synthase is expressed in cultured human bronchiolar epithelium. *J Clin Invest* 94: 2231–2236, 1994. doi:10.1172/JCI117585.
28. **Shin HW, Condorelli P, George SC.** Examining axial diffusion of nitric oxide in the lungs using heliox and breath hold. *J Appl Physiol (1985)* 100: 623–630, 2006. doi:10.1152/japplphysiol.00008.2005.
29. **Shin HW, George SC.** Impact of axial diffusion on nitric oxide exchange in the lungs. *J Appl Physiol (1985)* 93: 2070–2080, 2002. doi:10.1152/japplphysiol.00129.2002.
30. **Silkoff PE, McClean PA, Caramori M, Slutsky AS, Zamel N.** A significant proportion of exhaled nitric oxide arises in large airways in normal subjects. *Respir Physiol* 113: 33–38, 1998. doi:10.1016/S0034-5687(98)00033-4.
31. **Silkoff PE, McClean PA, Slutsky AS, Furlott HG, Hoffstein E, Wakita S, Chapman KR, Szalai JP, Zamel N.** Marked flow-dependence of exhaled nitric oxide using a new technique to exclude nasal nitric oxide. *Am J Respir Crit Care Med* 155: 260–267, 1997. doi:10.1164/ajrccm.155.1.9001322.
32. **Suresh V, Shelley DA, Shin HW, George SC.** Effect of heterogeneous ventilation and nitric oxide production on exhaled nitric oxide profiles. *J Appl Physiol (1985)* 104: 1743–1752, 2008. doi:10.1152/japplphysiol.01355.2007.
33. **Tsoukias NM, George SC.** A two-compartment model of pulmonary nitric oxide exchange dynamics. *J Appl Physiol (1985)* 85: 653–666, 1998. doi:10.1152/jappl.1998.85.2.653.
34. **Van Muylem A, Kerckx Y, Michils A.** Axial distribution of nitric oxide airway production in asthma patients. *Respir Physiol Neurobiol* 185: 313–318, 2013. doi:10.1016/j.resp.2012.09.011.
35. **Van Muylem A, Noël C, Paiva M.** Modeling of impact of gas molecular diffusion on nitric oxide expired profile. *J Appl Physiol (1985)* 94: 119–127, 2003. doi:10.1152/japplphysiol.00044.2002.
36. **Verbanck S, Kerckx Y, Schuermans D, Vincken W, Paiva M, Van Muylem A.** Effect of airways constriction on exhaled nitric oxide. *J Appl Physiol (1985)* 104: 925–930, 2008. doi:10.1152/japplphysiol.01019.2007.
37. **Weibel ER.** *Morphometry of the Human Lung*. New York: Academic, 1963. doi:10.1007/978-3-642-87553-3.